Journal of Power Sources 195 (2010) 1920–1925

Contents lists available at ScienceDirect

Journal of Power Sources

journal homepage: www.elsevier.com/locate/jpowsour

Y-substituted $SrTiO_3$–YSZ composites as anode materials for solid oxide fuel cells: Interaction between SYT and YSZ

Qianli Ma*, Frank Tietz, Doris Sebold, Detlev Stöver

Institute of Energy Research (IEF-1), Forschungszentrum Jülich GmbH, 52425 Jülich, Germany

ARTICLE INFO

Article history:
Received 22 June 2009
Received in revised form 30 July 2009
Accepted 26 September 2009
Available online 9 October 2009

Keywords:
Ceramic
Donor-doped strontium titanate
Solid oxide fuel cells
Anode material
Electrical conductivity

ABSTRACT

Donor-substituted $SrTiO_3$ ceramic materials were investigated as the anodes of solid oxide fuel cells (SOFCs). $Sr_{0.89}Y_{0.07}TiO_{3-\delta}$ (SYT) samples with good electrical conductivity and redox stability were prepared. The thermal and chemical expansions of SYT are both compatible with YSZ electrolyte. Half cells consisting of a flat anode substrate and an electrolyte layer with outer dimensions of 5 cm × 5 cm were fabricated, Ni particles were infiltrated on the pore walls within the ceramic anode framework, and the redox stability of the half cell was tested by He leakage tests after redox cycling. Ti diffusion but no Sr migration was found between the anode and electrolyte layers. $Sr_{0.895}Y_{0.07}Ti_xO_{3\pm\delta}$ (x = 1.00–1.20)–YSZ composites with a volume ratio 2:1 were prepared to investigate the influences of this interdiffusion between YSZ and SYT materials. The results indicate that the conductivity of SYT decreases because of the Ti diffusion, and a small amount of Ti excess can solve this problem.

1. Introduction

Donor-substituted $SrTiO_3$ materials have attracted increasing interest during the last few years as possible anode materials for solid oxide fuel cells (SOFCs), not only because of their high electrical conductivity after treatment in reducing atmosphere at high temperature [1–3], but, more importantly, because their thermal expansion is close to that of yttria-stabilized zirconia (YSZ) [3–5] and they have good dimensional stability upon redox cycling [3,4]. These properties are important advantages in comparison with the conventional Ni–YSZ cermet anode and other perovskite-based alternatives [6]. An anode-supported planar design is the most widely used concept for SOFCs today, especially for reduced operating temperatures [7], which is the tendency in the development of SOFCs because of the improved long-term stability of cells and integration of low-cost interconnect materials. Donor-substituted $SrTiO_3$ is very suitable for reduced operating temperatures because after heat treatment in reductive atmosphere it shows better conductivity at lower temperatures [3,8]. However, insufficient ionic conductivity and low electrocatalytic activity are the main drawbacks for donor-substituted $SrTiO_3$ anodes. In order to increase the ionic conductivity, mixed ceramics such as YSZ and donor-substituted $SrTiO_3$ are required for SOFC anodes [6,9]. Although no impurity phase has been observed by XRD after co-firing this ceramic mixture in air or in reductive atmosphere [1,4,10,11], element diffusion still may happen. For example, the formation of Ti-doped YSZ or $SrZrO_3$ is in doubt. The influence of these possible element diffusions on the properties of YSZ or ceramic composites has not been exhaustively investigated to date. It has been reported that the infiltration of small amounts of a catalyst, especially Ni infiltration, will be effective in increasing the electrocatalytic activity of donor-substituted $SrTiO_3$ anodes [4,6,12–14].

Numerous investigations have been reported for the donor-substituted $SrTiO_3$ itself. In very recent years, research has concentrated on evaluating the practical usage of these materials. Single cells were assembled with donor-substituted $SrTiO_3$-based anodes [3,10,15–18]. Some of them showed a remarkable power density of about 500 mW cm^{-2} at 800 °C [17,18], close to the level for practical application. However, the cells mentioned above were all based on small pellets fabrication, which is far from commercial requirements. In order to evaluate these materials more practically, a cell with dimensions of at least 5 cm × 5 cm should be used.

In this work, $Sr_{0.89}Y_{0.07}TiO_{3-\delta}$ (SYT) powder was prepared in large amount, the electrical properties of the powder were characterized. Anode-supported planar half cells with dimensions of 5 cm × 5 cm × 0.15 cm based on SYT materials were fabricated, the redox cycling behavior of such half cells was investigated, and the element diffusion between SYT and YSZ was analysed.

2. Experimental

2.1. Preparation and characterization of SYT

$Sr_{0.89}Y_{0.07}TiO_{3-\delta}$ (SYT) powder was prepared in large amount (1 kg per batch). Titanium (IV) isopropoxide (97%), $Sr(NO_3)_2$

* Corresponding author. Tel.: +49 2461 614596; fax: +49 2461 612455.
E-mail address: q.ma@fz-juelich.de (Q. Ma).

0378-7753/$ – see front matter © 2009 Elsevier B.V. All rights reserved.
doi:10.1016/j.jpowsour.2009.09.075

Table 1
List of samples.

Abbreviation	Nominal starting composition	Effective starting composition	Analysed final composition of YSZ in SYT*x*–YSZ
8YSZ	ZrO_2 + 8 mol% Y_2O_3	$Y_{0.148}Zr_{0.852}O_{1.926}$	–
SYT1.00	$Sr_{0.895}Y_{0.07}TiO_3$	$Sr_{0.895}Y_{0.07}TiO_3$	$Ti_{0.11}Y_{0.16}Zr_{0.73}O_{1.92}$
SYT1.05	$Sr_{0.895}Y_{0.07}Ti_{1.05}O_{3.1}$	$Sr_{0.852}Y_{0.067}TiO_{2.952}$	$Ti_{0.13}Y_{0.17}Zr_{0.68}O_{1.92}$
SYT1.10	$Sr_{0.895}Y_{0.07}Ti_{1.10}O_{3.2}$	$Sr_{0.814}Y_{0.064}TiO_{2.909}$	$Ti_{0.17}Y_{0.16}Zr_{0.67}O_{1.92}$
SYT1.15	$Sr_{0.895}Y_{0.07}Ti_{1.15}O_{3.3}$	$Sr_{0.778}Y_{0.061}TiO_{2.87}$	$Ti_{0.20}Y_{0.15}Zr_{0.65}O_{1.93}$
SYT1.20	$Sr_{0.895}Y_{0.07}Ti_{1.20}O_{3.4}$	$Sr_{0.746}Y_{0.058}TiO_{2.833}$	$Ti_{0.22}Y_{0.14}Zr_{0.64}O_{1.93}$

(99.9%), $Y(NO_3)_3{\cdot}6H_2O$ (99.9%) were used as starting materials. The titanium (IV) isopropoxide was dropped into distilled water while it was stirred. The precipitate was filtered and washed, and then dissolved into HNO_3 solution. The Ti^{4+} concentration in this solution was determined by thermal gravimetry. Corresponding amounts of the nitrates were then added to the solution. After homogenisation the solution was spray-pyrolysed in a commercial spray dryer (Nubilosa, Konstanz, Germany). After spray pyrolysis the raw powder was heated up to 900 °C in air for 5 h. XRD using a Siemens D5000 diffractometer with Cu Kα radiation showed that the powder was a pure perovskite after calcination. The powder was then uniaxially pressed into rectangular bars (40 mm × 5 mm × 3 mm) and sintered in Ar/4% H_2 at 1400 °C for 5 h. The relative densities of the bars were over 99% of the theoretical density. The electrical conductivity of the bars was measured by the DC four-probe method in the temperature range of 25–910 °C in Ar/4% H_2 with 3% H_2O. The thermal and chemical expansion behavior of the bars was measured using a push-rod dilatometer (Netzsch DIL 402C).

2.2. Preparation and characterization of SYT–YSZ half cells

The SYT was mixed with commercial 8YSZ powder ($Zr_{0.852}Y_{0.148}O_{1.926}$, Tosoh, Japan) in the volume ratio of 2:1 (1.7:1 in weight ratio) by 24 h ball milling (SYT–YSZ). The mixed powder or pure SYT powder was then coat-mixed and warm pressed [19] to plates with dimensions of 7 cm × 7 cm × 0.2 cm. After de-bindering and pre-sintering at 1250 °C in air, the plates were vacuum slip-cast with a YSZ electrolyte layer on the topside, then sintered in Ar/4% H_2 at 1400 °C for 5 h. The size of the plates after sintering was 5 cm × 5 cm × 0.15 cm with a YSZ layer thickness of 10 μm. The redox and mechanical stability of the sintered plates was indirectly tested by He leakage tests of the electrolyte. The ceramic structures of the sintered plates were impregnated with NiO by immersing the plates in Ni nitrate solution applying a vacuum pump to reduce the remaining air inside the pores of the substrate and subsequently heating the plates up to 600 °C. The microstructure of the as-prepared half cells was investigated by scanning electron microscopy (SEM, Zeiss Ultra55) and the composition in the YSZ layer was analysed by energy-dispersive X-ray spectroscopy (EDX).

2.3. Preparation and characterization of SYT*x*–YSZ

In order to investigate the interaction between SYT and YSZ, conductivities of the dense (over 95% relative density) SYT–YSZ bars (prepared by uniaxial pressing) and porous SYT bars (prepared by coat-mix and warm pressing, with porosity of 29%) were compared. In addition, SYT powders with 0–20 mol% Ti in excess were prepared by Pechini's method (see Table 1) [20]. After mixing with YSZ (in the volume ratio of 2:1, SYT*x*–YSZ, *x* = 1.00–1.20) and preparation with same processes as above, the relative densities of the samples were 86–99% of the theoretical density, which decrease with increasing Ti content.

3. Results and discussion

3.1. Electrical, physical and chemical properties of SYT

Fig. 1 shows the conductivity in reducing atmosphere and the redox stability of the SYT samples. The conductivity was 136 and 200 S cm^{-1} at 800 and 600 °C, respectively. After 3 redox cycles between Ar/4% H_2 and air at 600 °C, the conductivity decreased by 1.7%. It should be noted that the electrical conductivity of SYT depends to a very large extent on the preparation and processing procedures [8] leading to different porosity and concentration of Ti^{3+} ions. As a rough estimate, the target for the electronic conductivity for anode materials is set at 100 S cm^{-1} for low ohmic resistance of the fuel cell. However, the actual requirement depends on the cell design, and particularly on the length of the current path for current collection. Thus this requirement may be relaxed to as

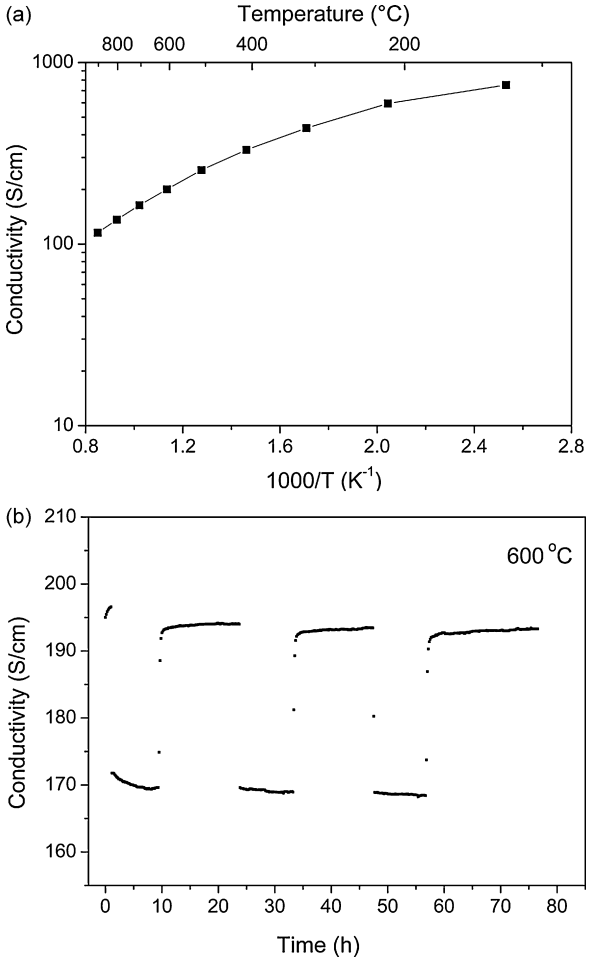

Fig. 1. Electrical properties of spray-dried and sintered powder of SYT: (a) temperature dependence of the conductivity in Ar/4% H_2 with 3% H_2O and (b) electrical conductivity during redox cycling at 600 °C between Ar/4%H_2 and air (both with 3% H_2O).

low as 1 S cm^{-1} [21]. In this case, the conductivity of SYT is about two orders of magnitude higher than the specified value for such SOFC anodes. It is also discussed [6] that during redox cycles of SYT samples, the equilibrium restoration upon change of $p(O_2)$ and temperature cannot be completed within reasonable measuring times due to the limitation of ion diffusion kinetics in the solid state, which is assumed to be the reason of 1.7% conductivity decrease in this work. Furthermore, it is predictable that longer reoxidation time, more redox cycles and higher redox temperature will enhance the decrease of conductivity. Further experiments are needed to investigate how these conditions will influence the redox performance of SYT anodes. According to this study, however, at least for SOFCs operated at intermediate temperature (around 600 °C), the redox stability of SYT is reasonably good. The thermal expansion coefficient of the sample was 11.8×10^{-6} K^{-1}, which is close to that of YSZ [22]. The chemical expansion of the SYT at 800 and 600 °C between wet Ar/4% H_2 and air was only 0.014 and 0.025%, respectively.

3.2. Ti diffusion in half cells

The SEM micrographs of the half-cell samples are shown in Fig. 2. The cross section view (Fig. 2a) shows the uniform 10-μm-thick YSZ layer with only a few closed pores and very good adherence to the SYT–YSZ anode substrate. Both YSZ and SYT are well connected to each other in the substrate. The NiO particles are evenly dispersed on the pore walls (Fig. 2b). On the one hand, these particles will ensure the electrocatalytic activity of the anode and, on the other hand, because of their amount and position, the dimensional change of the particles during the redox process will not affect the mechanical stability of the anode in contrast to NiO/YSZ cermets. The porosities of the manufactured anodes are around 30%, which is sufficient for fuel gas penetration.

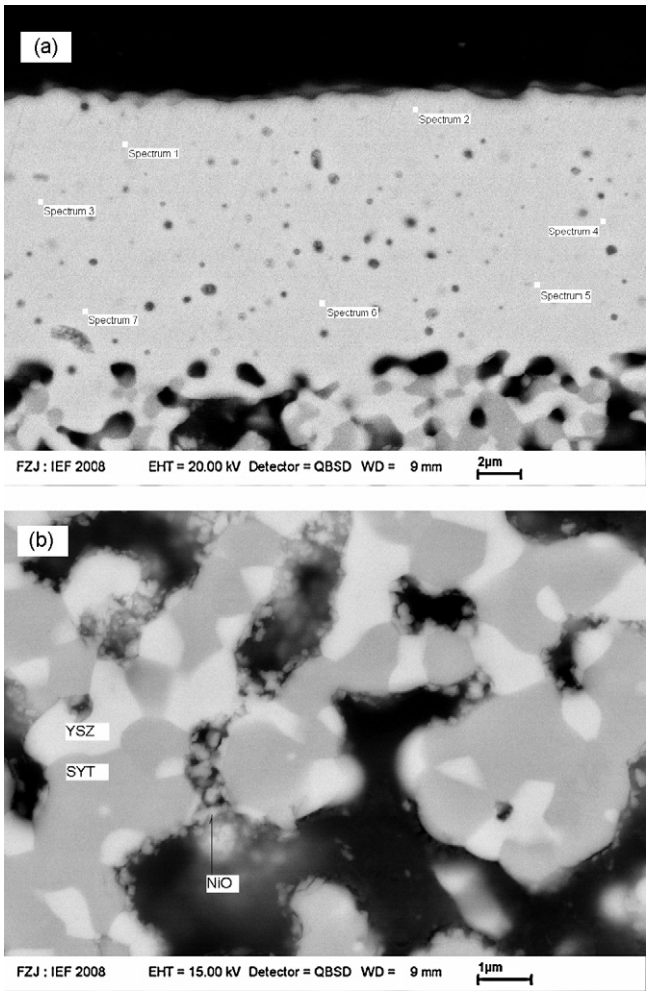

Fig. 2. Microstructure and element analysis of sintered half cells. (a) Cross section of SYT–YSZ/YSZ bilayer (spectrum 1–7 correspond to data listed in Table 2) and (b) NiO particles dispersed in the ceramic structure of SYT–YSZ.

Table 2
Element analysis (in at.%) by EDX of points indicated in Fig. 2a.

Spectrum no.	Ti	Sr	Y	Zr
Spectrum 1	4.0	0.0	14.0	82.0
Spectrum 2	3.5	0.0	12.0	84.5
Spectrum 3	4.0	0.0	14.5	81.5
Spectrum 4	4.5	0.0	12.0	83.5
Spectrum 5	6.0	0.0	12.5	81.5
Spectrum 6	6.0	0.0	13.5	80.5
Spectrum 7	5.0	0.0	13.0	82.0

EDX analysis was performed at different positions of the sintered SYT–YSZ/YSZ bilayers (Fig. 2a) and the corresponding element analysis is shown in Table 2. No Sr was found at any part of YSZ layer, indicating that no $SrZrO_3$ formation occurred during co-sintering of the anode or the concentration of $SrZrO_3$ is below the detection limit of EDX analysis. This could be beneficial for cell performance because the formation of $SrZrO_3$ would increase the area-specific resistance of the cells. About 3.5–6.0 mol% Ti was found in the YSZ layer, which indicates the existence of Ti diffusion from SYT to YSZ. A gradient of the Ti incorporation in the YSZ layer was observed, decreasing from the SYT–YSZ layer side to the opposite electrolyte surface.

Actually, Ti-doped YSZ has been widely investigated as a mixed conductor and also considered for use as the anode of SOFCs [23–30]. The solubility limit of TiO_2 in the YSZ fluorite was determined to be at least 10 mol% [23,27–30]. The ionic transport number for 10 mol% TiO_2-substituted YSZ sintered at 1500 °C in air is 0.78 at 1000 °C [27] indicating significant electronic conductivity. The electronic conductivity of the electrolyte will cause internal short-circuiting and decrease the open current voltage (OCV) and power density of the cell. According to the published results on SOFCs with doped $SrTiO_3$ anode and YSZ electrolyte [3,10,15–18], no obvious OCV decrease was found, which indicates that the diffusion of Ti in YSZ will not cause significant electronic conduction of YSZ. However, it should be noted that the cells formerly investigated either had a YSZ electrolyte thicker than 50 μm, which is probably too thick for Ti to diffuse from one side to another, or/and had a cathode-supported design, in which the doped $SrTiO_3$ anodes were only a thick film and sintered only at 1200 °C in air [17], which is limiting the Ti diffusion. Because here SYT is fabricated as an anode support at 1400 °C and the thickness of the YSZ layer is only 10 μm, the influence of Ti diffusion may be more pronounced. Single-cell performance tests are needed to investigate the influence of Ti diffusion into YSZ layer and the impact on OCV in more detail, and are in preparation at present.

3.3. The influence of Ti diffusion to SYT

Not only is the YSZ layer affected by Ti diffusion, but the electrical properties of SYT in the SYT–YSZ anode are also different from those of pure SYT. Fig. 3 compares the conductivity of dense (relative density >95%) SYT–YSZ (volume ratio 3:1, SYT3–YSZ1) and pure SYT with a porosity of 29 vol.%. Considering that YSZ has much lower electronic conductivity than SYT, SYT3-YSZ1 can be regarded as an SYT sample with a non-conductive phase or a porosity of 25 vol.%. If there is no interaction between SYT and YSZ in SYT3–YSZ1, this sample should have shown higher con-

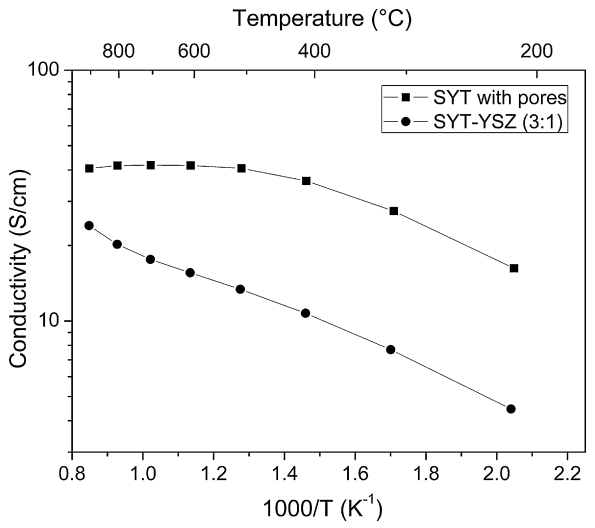

Fig. 3. Comparison of the conductivities of dense SYT–YSZ (3:1 in volume) and SYT with porosity of 29% in Ar/4% H_2 with 3% H_2O. Both samples have nearly the same volume of electronically non-conductive phase.

ductivity than the sample with 29 vol.% porosity, because actually YSZ has a limited conductivity in comparison to bare pores and the SYT sample has a higher porosity than the content of YSZ in the SYT3–YSZ1 sample. Instead, SYT shows much higher conductivity than SYT3–YSZ1 (see Fig. 3). The reason is most likely the Ti diffusion from SYT to YSZ. After the diffusion, the composition of SYT is significantly deviating from the initial composition of $Sr_{0.89}Y_{0.07}TiO_{3-\delta}$. In order to further confirm this assumption, the properties of $Sr_{0.895}Y_{0.07}Ti_xO_{3+\delta}$ (x = 1.00–1.20)–YSZ (volume ratio 2:1, SYTx–YSZ) were investigated.

Apart from perovskite and fluorite no other phases were observed by XRD in the SYTx–YSZ specimens after sintering at 1400 °C for 5 h in 4% H_2–Ar (Fig. 4a). No Ti-rich phase appeared even for highly A-site deficient samples like SYT1.15–YSZ and SYT1.20–YSZ (cf. Table 1). In contrast, the pure SYTx materials contained a Ti-rich phase ($x \geq 1.05$) as reported in [8], which indicates that the excess of Ti in SYTx enters the YSZ. A more specific comparison is shown in Fig. 4b. The reflections of SYT in SYTx–YSZ are almost at the same diffraction angle while those of YSZ are slightly shifted to larger angles with increasing amounts of Ti, indicating a decrease of the lattice parameter of YSZ in SYTx–YSZ from x = 1.00 to x = 1.20. The lattice parameter values are all smaller than that of pure YSZ

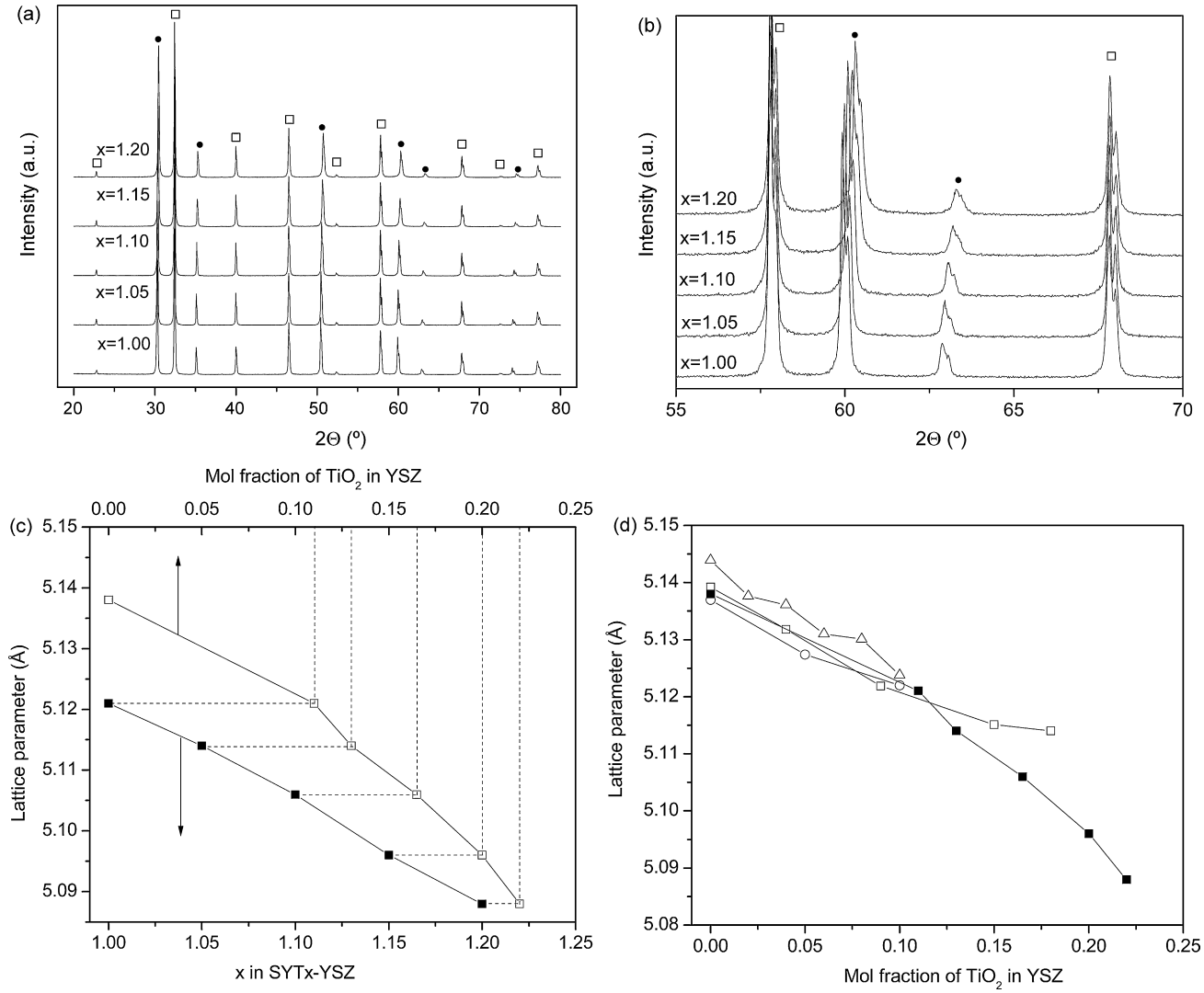

Fig. 4. (a) XRD patterns of SYTx–YSZ samples sintered in Ar/4%H_2 at 1400 °C for 5 h. Circles and squares indicate YSZ and $SrTiO_3$, respectively. (b) Partly enlarged view of (a). (c) Dependence of the lattice parameters of SYTx–YSZ samples on x value (closed square) and actual Ti content calculated from SEM-EDX results in YSZ phase (open square). (d) Comparison of the lattice parameter of Ti-containing YSZ between this work (closed square symbols) and data from Refs. [27,28,30] (open circle, triangle, and square symbols, respectively).

before sintering with SYT*x* (5.138 Å). This decrease has also been mentioned for other Ti-substituted YSZ materials [23,27–30]. Since the ionic radius of Ti^{4+} is smaller than that of Zr^{4+}, it is reasonable that the lattice parameter of YSZ decreases. According to Vegard's rule, the decrease of lattice parameter should be proportional to the actual Ti content in the YSZ phase of SYT*x*–YSZ. This has been confirmed by SEM-EDX measurements. In Fig. 4c the lattice parameters of YSZ in SYT*x*–YSZ samples determined from XRD are plotted versus the Ti excess in SYT*x* and show a linear dependence on the initial perovskite composition. In addition, the same lattice parameters are plotted versus the actual Ti content in YSZ measured by SEM-EDX. The mol fraction of Ti in YSZ clearly increases with the *x* value of SYT*x*–YSZ. Therefore also the lattice parameters of the YSZ phase decrease with the Ti content. Fig. 4d compares the lattice parameters of Ti-substituted YSZ of this work with previously reported results [27,28,30]. Up to 10 mol% Ti the lattice parameters in this study are in good agreement with the formerly measured data. At higher Ti contents the single phase region is extended to at least 22 mol% Ti and the lattice parameters are slightly smaller than reported in [30]. The reason for these two differences is probably the fact that the samples in this work were sintered in reducing atmosphere, while those in earlier reports [27,28,30] were sintered in air. It was reported that TiO_2-containing YSZ had an abnormal shrinkage of lattice parameters in reducing atmosphere [31]. Although a fraction of Ti^{4+} ions was reduced to Ti^{3+} and the ionic radius of Ti^{3+} is larger than that of Ti^{4+}, shrinkage of the lattice parameter was still found in Ti-substituted YSZ after sintering in reducing atmosphere, which is in agreement with the results of the present work.

Fig. 5 shows the conductivities of SYT*x*–YSZ samples in reducing atmosphere. Apparently, the conductivity increases with increasing *x* value in SYT*x*–YSZ up to $x = 1.10$. For the SYT*x*–YSZ samples with a lower *x* value ($x = 1.00, 1.05$), it is likely that the stoichiometry of SYT in SYT*x*–YSZ may have changed from A-site deficiency to B-site deficiency because of the Ti loss, while for the samples with a higher *x* value ($x = 1.10, 1.15, 1.20$) the SYT phase can still remain A-site deficient because enough Ti has been added to compensate the loss due to the diffusion into the YSZ phase. As widely agreed, A-site-deficient $SrTiO_3$ shows higher conductivity in reducing atmosphere than stoichiometric or B-site-deficient materials [2,8,32,33]. It is discussed [2] that the existence of A-site vacancies may weaken the bond strength in TiO_6 octahedra adjacent to the cation vacancies. When the material containing a large number of A-site vacancies is heated up in reducing atmosphere, the formation of Ti^{3+} occurs more easily and many oxygen vacancies plus electrons can be generated and the electrical conductivity is consequently increased.

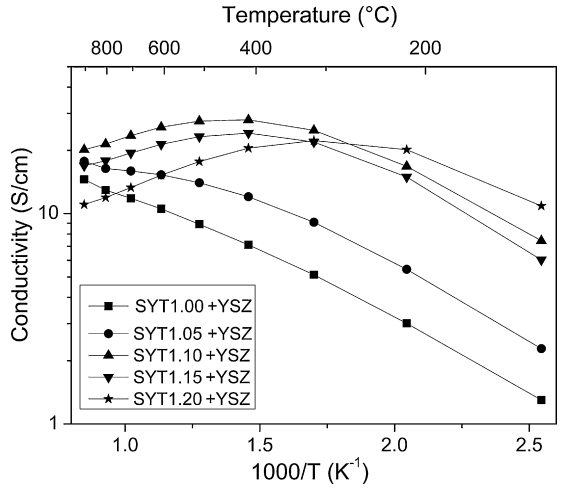

Fig. 5. Conductivities of SYT*x*–YSZ samples in Ar/4% H_2 with 3% H_2O.

Table 3
Calculated composition of SYT*x* in SYT*x*–YSZ.

Abbreviation	Calculated final composition of SYT in SYT*x*–YSZ
SYT1.00	$[Sr_{0.911}Y_{0.059}][Ti^{4+}_{0.877}Ti^{3+}_{0.030}]O_{2.80}$
SYT1.05	$[Sr_{0.926}Y_{0.050}][Ti^{4+}_{0.906}Ti^{3+}_{0.025}]O_{2.85}$
SYT1.10	$[Sr_{0.911}Y_{0.047}][Ti^{4+}_{0.906}Ti^{3+}_{0.042}Y_{0.012}]O_{2.87}$ [a]
SYT1.15	$[Sr_{0.898}Y_{0.048}][Ti^{4+}_{0.889}Ti^{3+}_{0.054}Y_{0.02}]O_{2.88}$
SYT1.20	$[Sr_{0.884}Y_{0.045}][Ti^{4+}_{0.898}Ti^{3+}_{0.071}Y_{0.032}]O_{2.87}$ [b]

[a] Y concentration on B-site was set to a value for equal (stoichiometric) site occupation.
[b] Y concentration on B-site was fixed to obtain full B-site occupation.

Mott [34] theoretically predicated a transition from semiconducting to metallic behavior. If the concentration of Ti^{3+} exceeds a critical value, then the extra electrons at Ti sites may enter the conduction band, and a transition from semiconducting to metallic behavior may occur. This 'Mott transition' has already been discussed for reduced or donor-doped $SrTiO_3$ by some reports afterwards [2,35–39]. For the SYT*x*–YSZ samples with $x = 1.10, 1.15, 1.20$, this transition is also observed showing metallic behavior in the range of 900–400 °C. In contrast, the conductivities of SYT1.00–YSZ and SYT1.05–YSZ decrease with decreasing temperature showing semiconducting behavior over the entire temperature range. For both samples, the formation of Ti^{3+} is more difficult because the SYT phase is certainly B-site-deficient. Therefore the concentration of Ti^{3+} is smaller than the 'critical value' and the specimens show semiconducting behavior. The results agree very well with Mott's theory as well as the analytical results. According to the SEM-EDX results, 10–22 mol% of Ti was found in the YSZ phase of SYT*x*–YSZ mixtures. In addition, compared to the original formula of YSZ, a small increase in the Y content was observed (cf. Table 1). Hence, the compositions of SYT*x* have significantly changed. Table 3 shows the resulting calculated compositions of SYT*x* after considering the Ti and Y diffusion as well as charge compensation. SYT1.00 and SYT1.05 both change from A-site to B-site deficiency, SYT1.10 is almost stoichiometric, while SYT1.15 and SYT1.20 remain A-site-deficient. In the latter three cases a partial B-site occupation with Y has to be assumed to be in accordance with the conductivity data. Actually, the ionic radius of Y^{3+} ion (~0.10 nm) is almost halfway between Sr^{2+} ion (~0.14 nm) and Ti^{4+} ion (~0.06 nm). Thus, theoretically Y^{3+} could be accommodated on either cation site in $SrTiO_3$ lattice. Zhi et al. have reported that a high solubility (~12.2 mol%) of Y was found at the Ti site of $Ba_{1-x}Y_xTiO_3$ after sintering at 1515 °C [40]. Li and Qu also found that Y can enter either A-site or B-site of $Ba_{0.62}Sr_{0.38}TiO_3$ ceramics [41], indicating Y occupation on B-site of $SrTiO_3$ is also possible.

Further Ti addition ($x > 1.10$) also leads to decreasing conductivity, which maybe because of the slight decrease of relative density for the samples (as discussed in Section 2, the relative density of sintered samples of SYT*x*–YSZ slightly decrease with increasing Ti content). But according to Hui and Petric [2], too much Sr deficiency in donor-doped $SrTiO_3$ will also cause a decrease in conductivity, which also may be the reason why the conductivity of SYT*x*–YSZ decreases for $x > 1.10$. It is also noticed that the maximum of conductivity shifts to lower temperatures for samples of $x > 1.10$, indicating the transition from semiconducting to metallic conduction is probably shifted in temperature because of higher concentration of A-site vacancies facilitating Ti^{3+} formation at lower temperatures. Considering SYT1.10–YSZ has the highest conductivity among the SYT*x*–YSZ series, it may be a better choice for SOFCs anodes.

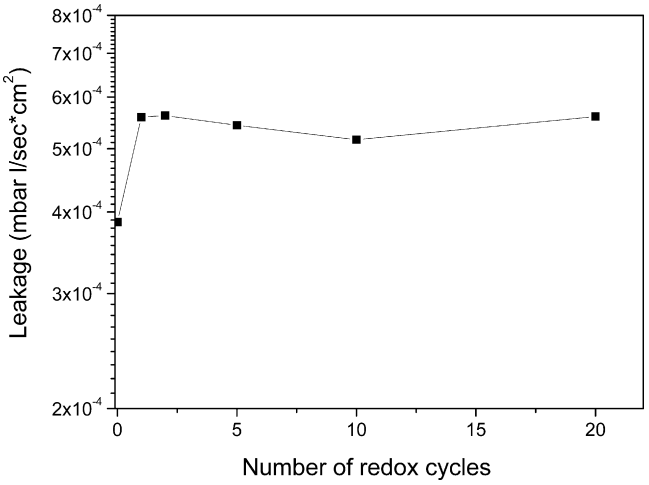

Fig. 6. Leakage test of sintered SYT–YSZ/YSZ bilayer after several redox cycles at 800 °C between air and Ar/4% H_2 (both with 3% H_2O). For each redox cycle the sample was exposed for 1 h in air and 23 h in Ar/H_2.

3.4. Redox stability of the half cells

Fig. 6 shows the He leakage values of sintered SYT–YSZ/YSZ bilayers after different redox cycles between air and Ar/4% H_2. For planar half cells based on NiO–YSZ anode and YSZ electrolyte, the threshold for gas-tightness is a He leakage rate of $<2 \times 10^{-5}$ mbar l/(s cm^2) [42], but after reduction of the anode to Ni–YSZ, the decease of He leak rate is normally 1–2 orders of magnitude [43]. In this case, the He leakage rate after 20 redox cycles with about 6×10^{-4} mbar l/(s cm^2) is significantly below the value of Ni–YSZ/YSZ half cells. More importantly, there is no obvious increase of leakage after 20 redox cycles although there is a small change after the first redox cycle, which is in accordance with earlier work [3,4] and proves the redox and mechanical stability of the prepared SYT–YSZ/YSZ bilayers.

4. Conclusions

SYT shows electrical conductivity of 136 S cm^{-1} at 800 °C and 200 S cm^{-1} at 600 °C in wet Ar/4%H_2 after reduction at 1400 °C. After three redox cycles between Ar/4% H_2 and air at 600 °C, the conductivity only decreased by 1.7%. The thermal and chemical expansions of SYT are both compatible with YSZ electrolyte. 5 cm × 5 cm half cells of Ni-infiltrated SYT–YSZ/YSZ with good microstructures were fabricated. According to the He leakage test, they had satisfactory dimensional stability upon redox cycling and did not show any damage to the electrolyte. No Sr diffusion was found between the SYT–YSZ and YSZ layers, but 3.5–6 at.% of Ti was found in the electrolyte. This diffusion may cause electronic conduction of YSZ and has been observed to decrease the conductivity of SYT in the SYT–YSZ composite. The addition of extra TiO_2 to SYT was found to decrease the lattice parameter of YSZ phase in SYT*x*–YSZ samples. This addition can also significantly increase the conductivity of SYT–YSZ composites adding up to 10 mol% of TiO_2. Because of the resulting low conductivity of SYT–YSZ after sintering, half cells of SYT substrate/SYT1.10–YSZ (~5–10 μm)/YSZ may be a better choice for further developments. Experiments addressing this issue are now in progress.

Acknowledgements

The authors thank Dr. W. Fischer (FZJ-IEF1) and Mr. M. Ziegner (FZJ-IEF 2) for XRD measurements, and the whole technical staff of FZJ-IEF1 for experimental assistance. Financial support from the European Commission under contract no. SES6-CT-2006-020089 of the Integrated Project "SOFC600" is gratefully acknowledged.

References

[1] H. Zhao, F. Gao, X. Li, C. Zhang, Y. Zhao, Solid State Ionics 180 (2009) 193–197.
[2] S.Q. Hui, A. Petric, J. Electrochem. Soc. 149 (2002) J1–J10.
[3] O.A. Marina, N.L. Canfield, J.W. Stevenson, Solid State Ionics 149 (2002) 21–28.
[4] Q.X. Fu, F. Tietz, D. Sebold, S.W. Tao, J.T.S. Irvine, J. Power Sources 171 (2007) 663–669.
[5] D. de Ligny, P. Richet, Phys. Rev. B 53 (1996) 3013–3022.
[6] Q.X. Fu, F. Tietz, Fuel Cells 8 (2008) 283–293.
[7] L.G.J. de Haart, K. Mayer, U. Stimming, I.C. Vinke, J. Power Sources 71 (1998) 302–305.
[8] Q.X. Fu, S.B. Mi, E. Wessel, F. Tietz, J. Eur. Ceram. Soc. 28 (2008) 811–820.
[9] T. Kolodiazhnyi, A. Petric, J. Electroceram. 15 (2005) 5–11.
[10] H.P. He, Y.Y. Huang, J.M. Vohs, R.J. Gorte, Solid State Ionics 175 (2004) 171–176.
[11] T. Nakamura, T. Kobayasia, K. Yashiroa, A. Kaimai, T. Otake, K. Sato, J. Mizusaki, T. Kawada, J. Electrochem. Soc. 155 (2008) B563–B569.
[12] S. Primdahl, Y.L. Liu, J. Electrochem. Soc. 149 (2002) A1466–1472.
[13] H. Uchida, S. Suzuki, M. Watanabe, Electrochem. Solid-State Lett. 6 (2003) A174.
[14] J. Liu, B.D. Madsen, Z.Q. Ji, S.A. Barnett, Electrochem. Solid-State Lett. 5 (2002) A122–124.
[15] X.L. Huang, H.L. Zhao, W.H. Qiu, W.J. Wu, X. Li, Energy Convers. Manage. 48 (2007) 1678–1682.
[16] S.Q. Hui, A. Petric, J. Eur. Ceram. Soc. 22 (2002) 1673–1681.
[17] H. Kurokawa, L.M. Yang, C.P. Jacobson, L.C. De Jonghe, S.J. Visco, J. Power Sources 164 (2007) 510–518.
[18] G.T. Kim, M.D. Gross, W.S. Wang, J.M. Vohs, R.J. Gorte, J. Electrochem. Soc. 155 (2008) B360–B366.
[19] D. Simwonis, H. Thülen, F.J. Dias, A. Naoumidis, D. Stöver, J. Mater. Process. Technol. 92/93 (1999) 107–111.
[20] M.P. Pechini, U.S. Patent No. 3,330,697, (1967).
[21] A. Atkinson, S. Barnett, R.J. Gorte, J.T.S. Irvine, A.J. McEvoy, M. Mogensen, S.C. Singhal, J.M. Vohs, Nat. Mater. 3 (2004) 17–27.
[22] F. Tietz, Ionics 5 (1999) 129–139.
[23] S.S. Liou, W.L. Worrell, Appl. Phys. A 49 (1989) 25–31.
[24] K. Kobayashi, Y. Kai, S. Yamaguchi, N. Fukatsu, T. Kawashima, Y. Iguchi, Solid State Ionics 93 (1997) 193–199.
[25] K. Kobayashi, K. Kato, T. Kawashima, S. Yamaguchi, Y. Iguchi, J. Ceram. Soc. Jpn. 106 (1998) 1073–1078.
[26] K.E. Swider, W.L. Worrell, J. Electrochem. Soc. 143 (1996) 3706–3711.
[27] M.T. Colomer, J.R. Jurado, J. Solid State Chem. 165 (2002) 79–88.
[28] M. Mori, Y. Hiei, H. Itoh, G.A. Tompsett, N.M. Sammes, Solid State Ionics 160 (2003) 1–14.
[29] F. Tietz, I. Arul Raj, D. Stöver, Br. Ceram. Trans. 103 (2004) 202–210.
[30] A.J. Feighery, J.T.S. Irvine, D.P. Fagg, A. Kaiser, J. Solid State Chem. 143 (1999) 273–276.
[31] F. Tietz, W. Jungen, P. Lersch, M. Figaj, K.D. Becker, D. Skarmoutsos, Chem. Mater. 14 (2002) 2252–2257.
[32] S. Komornicki, S. Kozinski, B. Mirek, M. Rekas, Solid State Ionics 42 (1990) 7–13.
[33] F. Gao, H. Zhao, X. Li, Y. Cheng, X. Zhou, F. Cui, J. Power Sources 185 (2008) 26–31.
[34] N.F. Mott, Rev. Mod. Phys. 40 (1968) 677–683.
[35] A. Fujimori, A.E. Bocquet, K. Morikawa, K. Kobayashi, T. Saitoh, Y. Tokura, I. Hase, M. Onoda, J. Phys. Chem. Solids 57 (1996) 1379–1384.
[36] I. Kim, T. Nakamura, Y. Inaguma, M. Itoh, J. Solid State Chem. 113 (1994) 281–288.
[37] Y. Tokura, Y. Taguchi, Okada, T. Arima, K. Kumagai, Y. Iye, Phys. Rev. Lett. 70 (1993) 2126–2129.
[38] J.E. Sunstrom IV, S.M. Kauzlarich, P. Klavins, Chem. Mater. 4 (1992) 346–353.
[39] R. Moos, K.H. Härdtl, J. Am. Ceram. Soc. 78 (1995) 2569–2571.
[40] J. Zhi, A. Chen, Y. Zhi, P.M. Vilarinho, J. Baptista, J. Am. Ceram. Soc. 82 (1999) 1345–1348.
[41] Y. Li, Y. Qu, Mater. Chem. Phys. 110 (2008) 155–159.
[42] R. Mücke, N.H. Menzler, H. Buchkremer, D. Stöver, ECS Trans. 7 (2007) 2175–2185.
[43] E. Wanzenberg, F. Tietz, P. Panjan, D. Stöver, Solid State Ionics 159 (2003) 1–8.